

## Friction in Adhesion

Bi-min Zhang Newby and Manoj K. Chaudhury\*

Department of Chemical Engineering and Polymer Interface Center, Lehigh University,  
Bethlehem, Pennsylvania 18015

Received March 11, 1998. In Final Form: June 12, 1998

The effect of interfacial friction on adhesion was studied by using a model system, in which a thin strip of silicone elastomer was peeled from a PDMS (poly(dimethylsiloxane)) treated glass slide. The fluorescent particle tracking method revealed that the elastomer stretches and slides on glass well before the crack faces open up. Interfacial energy dissipation due to friction, which is the product of the slip displacement and the interfacial shear stress, is found to be a significant contributor to the total fracture energy at various peel configurations. These results suggest that interfacial sliding may provide a mechanism for energy dissipation in the fracture of asymmetric interfaces.

### Introduction

Fracture occurs at the interface of two materials when the mechanically applied energy (fracture energy,  $G$ ) per unit extension of crack area is equal to or greater than the thermodynamic work of adhesion ( $W_A$ ). The fracture energy of a real system is generally a rate dependent quantity, which can be several orders of magnitude higher than the thermodynamic work of adhesion. In these cases, the excess energy ( $G - W_A$ ) is dissipated by a viscoelastic mechanism operating at or near the crack tip region.

$$G - W_A = T\dot{s}/V \quad (1)$$

where  $V$  is the crack velocity and  $T\dot{s}$  is the energy dissipation per unit crack width. Several authors<sup>1–7</sup> have argued that the energy dissipation per unit extension of crack area ( $T\dot{s}/V$ ) can be expressed as a product of the thermodynamic work of adhesion ( $W_A$ ) and a function  $\Phi$ , characterizing the rheological deformations of the materials, i.e.

$$G - W_A = W_A \Phi \quad (2)$$

For viscoelastic polymers, the maximum value of  $\Phi$  can be as large as the ratio of the polymer's glassy modulus to its relaxed modulus;<sup>4–7</sup> hence, considerable amplification of fracture energy is possible in viscoelastic systems.

Equation 2 simplifies the problem of viscoelastic crack considerably by separating the effects produced by the interfacial and bulk rheological forces. Recent studies are, however, pointing out that the actual problem of crack propagation is far more complex than originally thought, because the processes occurring at the interface may be rate dependent. Such rate dependent interfacial processes may involve pull-out of polymer chains,<sup>8–12</sup> chemical

reaction,<sup>13</sup> and shear-induced slippage at the interface.<sup>14–15</sup> The objective of this paper is to show that the interfacial friction provides a mechanism for energy dissipation in many systems.

According to linear elastic fracture mechanics, the applied force is distributed as normal ( $\sigma_I$ ) and shear ( $\sigma_{II}$ ) stresses near the crack tip region as follows:

$$\sigma_I = \frac{K_I}{\sqrt{2\pi r}} \quad (3)$$

$$\sigma_{II} = \frac{K_{II}}{\sqrt{2\pi r}} \quad (4)$$

where  $K_I$  and  $K_{II}$  are the mode I (normal) and mode II (shear) stress intensity factors, the magnitudes of which depend on the level of remote stress, geometry of the system and the mode of application of stress.

The relative importance of both the fracture modes has previously been described in terms of a phase angle,<sup>16–17</sup> which is defined as  $\psi = \tan^{-1}(K_{II}/K_I)$ . The phase angle is zero (i.e., no shear), when a crack propagates in a purely isotropic and homogeneous medium. However, when dissimilar materials are involved,<sup>16</sup> i.e., in adhesive situations, a shear stress may develop at the interface. Shear stress also develops if the thickness<sup>16</sup> of one of the materials is different from the other or when two identical materials are fractured in an asymmetric fashion (Figure 1).

In the continuum mechanics description, the interfacial force acts as a Dirac force, which supports the stress singularity at the crack tip.<sup>18</sup> Barenblatt<sup>19</sup> showed that

(10) Creton, C.; Brown, H. R.; Shull, K. R. *Macromolecules* **1994**, *27*, 3174.

(11) Brown, H. R.; Hui, C.-Y.; Raphael, E. *Macromolecules* **1994**, *27*, 608.

(12) Deruelle, M.; Leger, L.; Tirrell, M. *Macromolecules* **1995**, *28*, 7419.

(13) Krausz, A. S.; Krause, K. *Fracture Kinetics of Crack Growth*; Kluwer Academic Publishers: Dordrecht, The Netherlands, 1988.

(14) Zhang Newby, B.-m.; Chaudhury, M. K.; Brown, H. R. *Science* **1995**, *269*, 1407.

(15) Zhang Newby, B.-m.; Chaudhury, M. K. *Langmuir* **1997**, *13*, 1805.

(16) Hutchinson, J. W.; Suo, Z. *Adv. Appl. Mech.* **1992**, *29*, 63.

(17) Thouless, M. D.; Jensen, H. M. *J. Adhesion* **1992**, *38*, 185.

(18) Maugis, D. In *Adhesive Bonding*; Lee, L.-H., Ed.; Plenum Press, New York, 1991; p 307.

(19) Barenblatt, G. I. *Adv. Appl. Mech.* **1962**, *7*, 55.

\* To whom correspondence should be addressed.

(1) Gent, A. N.; Kinloch, A. J. *J. Polym. Sci.* **1971**, *A2* (9), 659.

(2) Gent, A. N.; Schultz, J. *J. Adhesion* **1972**, *3*, 281.

(3) Andrews, E. M.; Kinloch, A. J. *Proc. R. Soc. London* **1973**, *A332*, 385.

(4) Greenwood, J. A.; Johnson, K. L. *Philos. Mag.* **1981**, *A43* (3), 697.

(5) de Gennes, P. G. *C. R. Acad. Sci. Paris* **1988**, *307* (II), 1949.

(6) Hui, C.-Y.; Xu D.-B.; Kramer, E. J. *J. Appl. Phys.* **1992**, *72* (8), 3294.

(7) Xu, D.-B.; Hui, C.-Y.; Kramer, E. J. *J. Appl. Phys.* **1992**, *72* (8), 3305.

(8) Brown, H. R. *Science* **1994**, *263*, 1411.

(9) Brown, H. R. *Macromolecules* **1993**, *26*, 1666.

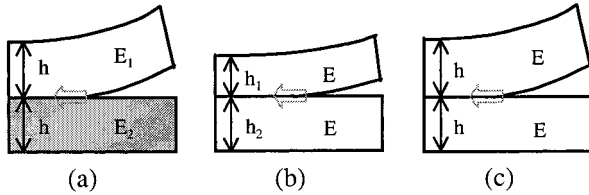


**Figure 1.** Shear stress may develop at and near the crack tip region in any of these asymmetric systems.  $E$  is the elastic modulus, and  $h$  is the film thickness.

the singularity of the normal stress is removed when one takes into account of the fact that the molecular restraining force is spread out in a cohesive zone ahead of the crack. Singularity of shear stress may be removed if micro slip<sup>20</sup> occurs near the crack tip. As the applied stress increases, the micro slip regions nucleate and spread over a large area.<sup>21</sup> When the interface can no longer support the applied stress, the crack faces may slide against each other with a concomitant energy dissipation at the interface.

An experimental verification of the role of friction in adhesion suffers from the difficulty that the interfacial shear stress is not always known a priori. Furthermore, it is difficult to detect and measure interfacial slip at the crack tip region. In this paper, we have used a model system, in which a thin elastomeric film is peeled from a low friction solid substrate. The extent of the slippage, in this case, was significant, so that it could be measured using a fluorescent particle tracking method.<sup>15</sup> These measurements allowed accurate estimation of the interfacial energy dissipation, which could then be compared with the total fracture energy.

## Results and Discussions

**Adhesion Studies with Model Systems.** In this section, we describe the results of peeling a thin ( $\sim 0.75$  mm) ribbon of silicone elastomer from a thin ( $\sim 100$  Å) film of poly(dimethylsiloxane) (PDMS) supported onto a glass slide. The adhesive fracture energy ( $G$ ) was calculated from the peel force per unit width ( $P$ ) according to the following equation.<sup>22</sup>

$$G = \frac{P^2}{2Eh} + P(1 - \cos \theta) \quad (5)$$

where  $\theta$  is the peel angle, and  $E$  and  $h$  are, respectively, the elastic modulus and the thickness of the silicone elastomer. The first term in eq 5 arises from the stretching of the elastic film, which accounts for most of the fracture energy at low peel angles ( $< 0.1$  rad). The second term is due to the bending stress in the film, which generally dominates the fracture energy at high peel angles.

The peel force and fracture energy increase with peel velocity and are shown in Figure 2. Although the thermodynamic work of adhesion ( $W_A$ ) between two PDMS surfaces is about  $47$  mJ/m<sup>2</sup>, the fracture energies obtained at two peel angles ( $5^\circ$  and  $40^\circ$ ) are 2–3 orders of magnitude greater than  $W_A$ . Evidently, the work of adhesion plays only a very small part in the total fracture energy. Hence, other mechanisms should be considered in order to explain the discrepancy.

Let us now examine what happens to a thin elastic ribbon being peeled from a rigid substrate at a low peel

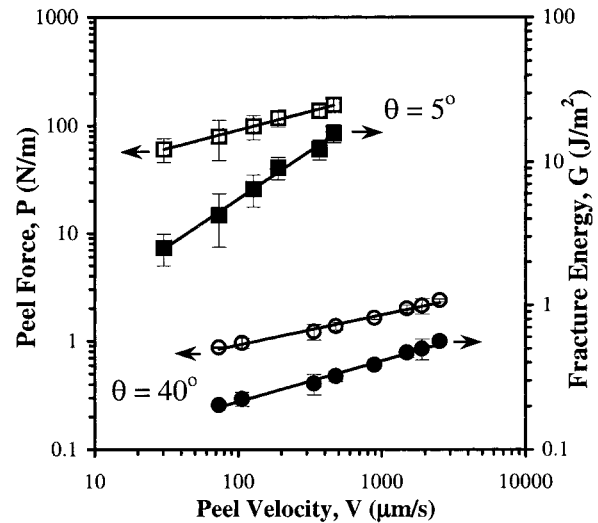


**Figure 2.** Peel force and the fracture energy of a PDMS elastomer on a PDMS-grafted glass surface increase with velocity.  $\square$  and  $\blacksquare$  denote the  $5^\circ$  peel angle, whereas  $\circ$  and  $\bullet$  denote the  $40^\circ$  peel angle, respectively. Peel forces ( $P$ , N/m) vary with velocity ( $V$ ,  $\mu\text{m/s}$ ) as follows:  $P = 18.6V^{0.35}$  at  $5^\circ$  peel and  $P = 0.253V^{0.28}$  at  $40^\circ$  peel, respectively. Fracture energies ( $G$ , J/m<sup>2</sup>) increase as follows:  $G = 0.25V^{0.67}$  at  $5^\circ$  peel and  $G = 0.058V^{0.28}$  at  $40^\circ$  peel, respectively. In both cases, the measured energies are significantly higher than the thermodynamic work of adhesion of PDMS ( $47$  mJ/m<sup>2</sup>).

angle (i.e.,  $5^\circ$ ). According to the theories of classical fracture mechanics, the elastomer separates from the substrate due to a bending moment near the crack tip,<sup>16–17</sup> overcoming the intermolecular forces. After separation, the elastomer stretches. In our case, since the interfacial friction is low, it is highly possible that the elastomer starts stretching and sliding even before it separates from the substrate. In that case, a substantial amount of energy can be dissipated by the frictional work at the interface. We will demonstrate that this frictional energy dissipation is a major contributor to the high fracture energy obtained in the above peel experiments. To build the background needed to compute the frictional energy dissipation, we first present a simple mechanical model<sup>23</sup> that describes the interfacial slip profile as a function of distance from the crack tip and then describe a method to measure it experimentally.

**Peel Mechanics with Interfacial Slip.** Figure 3 shows a thin cross section of the elastomer in contact with the substrate that is subjected to a tensile force. The elastic tension tends to stretch the strip, while interfacial friction prevents it. A force balance on a thin cross section yields the following equation:

$$\frac{\partial \sigma_{xx}}{\partial x} = \frac{\sigma_{yx}}{h} \quad (6)$$

where  $\sigma_{xx}$  is the elastic stress and  $\sigma_{yx}$  is the shear stress at the interface. The elastic stress,  $\sigma_{xx}$ , is given as follows:

$$\sigma_{xx} = E(\partial u / \partial x) \quad (7)$$

where  $E$  is the elastic modulus of the film and  $u$  is the elastic displacement. In an ideal case, the interfacial shear stress varies linearly with sliding velocity:

$$\sigma_{yx} = kv \quad (8)$$

(20) Mindlin, R. D. *Trans. ASME J. Appl. Mech.* **1949**, *16*, 259.

(21) Rice, J. R. *J. Mech. Phys. Solids* **1992**, *40* (2), 239.

(22) Kendall, K. *J. Phys. D: Appl. Phys.* **1975**, *8*, 1449.

(23) This treatment was suggested by Professor de Gennes.

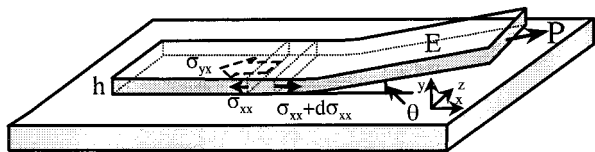


**Figure 3.** Sketch of an elastic ribbon peeling from a surface at a very low angle. A thin section of the ribbon experiences an elastic tensile stress ( $\sigma_{xx}$ ) and an interfacial shear stress ( $\sigma_{yx}$ ). The force balance on a differential cross section of the ribbon gives the equation for slip displacement (see eq 12).

where  $k$  is a kinetic friction constant and  $v$  is the slip velocity, which at steady state becomes

$$v = V(\partial u / \partial x) \quad (9)$$

In the above equation,  $V$  is the crack growth velocity measured with respect to the laboratory frame and  $u$  is the slip displacement at a distance  $x$  from the crack tip.

Combination of eqs 6–9 yields a steady-state diffusion equation for the displacement,  $u$ , as follows:

$$V(\partial u / \partial x) = hE/k(\partial^2 u / \partial x^2) \quad (10)$$

Shear stresses, for most real systems, however, vary with velocity in a nonlinear way, i.e.:

$$\sigma_{yx} = kV^n \quad (11)$$

In this case, slip displacement can be described by a nonlinear diffusion equation:

$$\left(\frac{\partial u}{\partial x}\right)^n = \frac{Eh}{kV^n} \left(\frac{\partial^2 u}{\partial x^2}\right) \quad (12)$$

Integration of eq 12 using the boundary conditions of  $u = 0$  at  $x = x_m$  (cutoff length), and  $E(\partial u / \partial x)_0 = P/h$  at  $x = 0$ , yields a relationship between  $u$  and  $x$  as follows:

$$u = \frac{(1-n)}{B(2-n)} [(A - Bx_m)^{2-n/1-n} - (A - Bx)^{2-n/1-n}] \quad (13)$$

where  $A = (\partial u / \partial x)_0^{1-n} = (P/Eh)^{1-n}$ , and  $B = (1-n)kV^n/Eh$ .

**Measurement of Interfacial Shear Stress from Peel Measurements.** The slippage of the elastic film on the PDMS grafted glass slide was studied according to a particle tracking method described previously.<sup>15</sup> Small fluorescent particles ( $\sim 0.5 \mu\text{m}$ ) were randomly deposited on one surface of the elastomer before placing it in contact with the glass slide. When the elastomer was peeled from the glass slide, the lateral movements of the particles were examined with a fluorescent microscope and videotaped. The slip profile was later examined in detail with a computer. Huge slippage of the elastomer occurred on the PDMS-modified glass slide at a peel angle of  $5^\circ$  (Figure 4). In all cases, the particles moved toward the crack with an average displacement of about  $100\text{--}120 \mu\text{m}$ . The slip profiles obtained at various peel velocities could be fitted with eq 13 very well, with a value of  $n \sim 0.36$ . This is the same as the exponent of the velocity found in the peel force measurement at  $5^\circ$  peel angle. The variation of the shear stress ( $\sigma(v)$ ) with slip velocity ( $v$ ), as obtained from the analysis of the above data, is shown in Figure 5. Notably, the interface exhibits a shear thinning behavior with an exponent (0.36) similar to that ( $\sim 1/3$ ) found earlier by others<sup>24–27</sup> for confined liquids.

**Shear Stress from Sliding Experiments.** In the above section, a convenient method is described that yields the interfacial shear stress between a PDMS elastomer

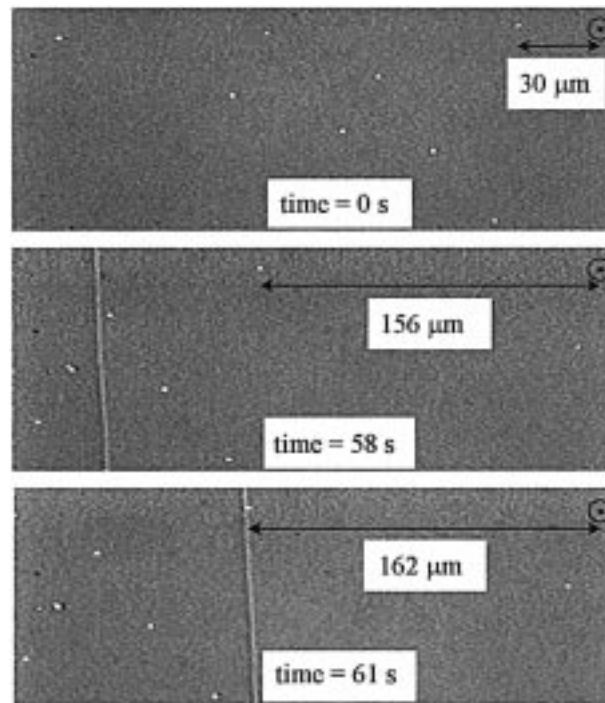


**Figure 4.** Video prints demonstrating the interfacial slippage of an elastic thin ( $\sim 0.75 \text{ mm}$ ) ribbon peeling from the PDMS-grafted glass surface at a  $5^\circ$  peel angle. The crack propagates from left to right. The fluorescent particles ( $0.5 \mu\text{m}$ ) present at the adhesive–substrate interface are seen as bright spots. To increase the visual clarity, the brightness of the particles has been enhanced with a computer. The black dots (circled) are artificially placed on the prints in order to provide fixed reference points for measuring the slip distances. When the crack propagates, the particles are seen to exhibit visible movement on the surface of PDMS. Particles start to move when they are as far as  $2 \text{ mm}$  away from the crack tip. One of the particles is seen to move by a net distance of  $129 \mu\text{m}$  laterally before it enters the crack tip.

and a PDMS film as a function of slip velocity. We now discuss how these values compare with the shear stresses measured by sliding hemispherical lenses on flat surfaces—a method first pioneered by Roberts and Tabor<sup>28</sup> and used later by others.<sup>8,29–33</sup> Here we have used a method similar to that of Brown,<sup>8</sup> in which a cantilever spring supporting a PDMS lens was deflected in such a way that the lens was dragged over the PDMS-grafted glass surface until the spring recovered its neutral position. The deflection of the spring yielded the friction force, which divided by the contact area gave the interfacial shear stress. We observed that the interfacial shear stress is independent of the contact area (range  $0.1\text{--}0.3 \text{ mm}^2$ ), as was also found by Homola et al.<sup>34</sup> in experiments using a surface force apparatus. The magnitudes of the shear stress at different velocities are in good agreement with the values obtained by Brown,<sup>8</sup> but they are about 60% lower than the values

(24) Granick, S. *Science* **1991**, *253*, 1374.

(25) Hu, H.-W.; Carson, G. A.; Granick, S. *Phys. Rev. Lett.* **1991**, *66*, 2758.

(26) Thompson, P. A.; Grest, G. S.; Robbins, M. O. *Phys. Rev. Lett.* **1992**, *68*, 3448.

(27) Robbins, M. O.; Smith, E. D. *Langmuir* **1996**, *12*, 4543.

(28) Roberts, A. D.; Tabor, D. *Proc. R. Soc. London* **1971**, *A325*, 323.

(29) Richards, S. C.; Roberts, A. D. *J. Phys.* **1992**, *D25*, A76.

(30) Savkoor, A. R.; Briggs, G. A. D. *Proc. R. Soc. London* **1977**, *A356*, 103.

(31) Briggs, G. A. D.; Briscoe, B. J. *Wear* **1975**, *35*, 357.

(32) Barquins, M. *Mater. Sci. Eng.* **1985**, *73*, 45.

(33) Chaudhury, M. K.; Owen, M. J. *Langmuir* **1993**, *9*, 29.

(34) Homola, A. M.; Israelachvili, J. N.; McGuiggan, P. M.; Gee, M. L. *Wear* **1990**, *136*, 65.

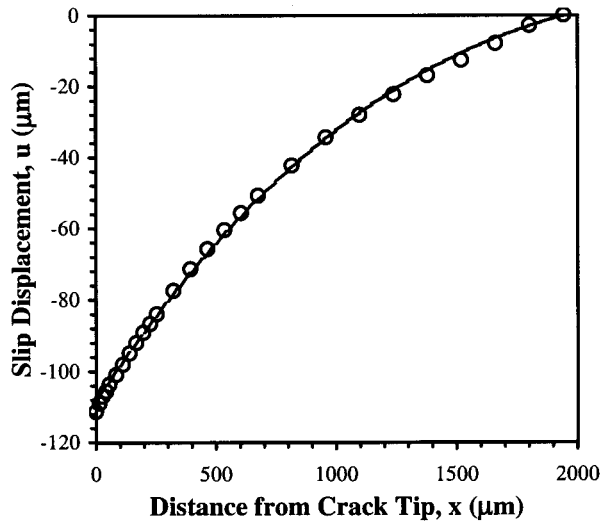


**Figure 5.** Slip displacement ( $u(x)$ ) of a fluorescent particle as a function of its distance ( $x$ ) from the crack tip. The experimental data ( $\circ$ ) fits with eq 13 very well. The fitting parameters are  $k = 2 \times 10^4$  and  $n = 0.36$  (see eqs 11 and 13). These data yield the interfacial shear stress between the PDMS elastomer and PDMS-grafted glass as  $\sigma = 2 \times 10^4 v^{0.36}$ , where  $\sigma$  and  $v$  are expressed as  $\text{N/m}^2$  and  $\mu\text{m/s}$ , respectively.

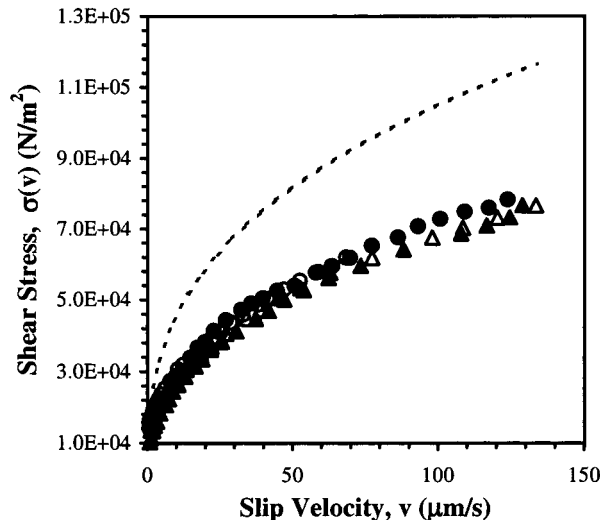


**Figure 6.** The interface between the elastic film and the PDMS-grafted surface exhibits a shear thinning behavior.  $\Delta$  and  $\blacktriangle$  represent the friction data obtained by sliding a hemispherical PDMS elastomer on a PDMS-grafted glass slide at contact areas of 0.25 and 0.31  $\text{mm}^2$ , respectively.  $\circ$  and  $\bullet$  are the shear stresses obtained by a modified method (see Figure 7) at contact areas 0.21 and 0.30  $\text{mm}^2$ , respectively. The dotted line represents the shear stress obtained from the analysis of slip data in peel experiments (see Figure 5).

obtained from the peel measurements (Figure 6). To verify if the reason for this discrepancy is due to the differences in quality of the PDMS surfaces used for the peel and sliding measurements, we have modified the above experiment in such a way that the surface of the elastomer that was used for the peel test could also be used for the sliding measurements (see Figure 7).

The magnitudes of the shear stresses for this system are still found to be similar to those of the sliding hemispheres, but lower than those obtained from the peel study (Figure 6). This proves that the differences between the frictional forces in the peel and the sliding experiments are not due to the differences in the surface properties of the elastomer. We are thus left with the possibility that the differences in the measured interfacial shear stresses

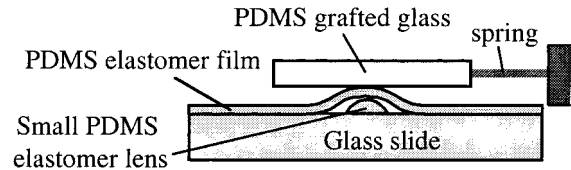


**Figure 7.** Sketch illustrating how the interfacial shear stress is measured with a PDMS ribbon that is also used in the peel experiments. The elastomer used for peel measurements was placed over a small (0.6 mm) PDMS lens. The central part of the elastomer formed a spherical nub just above the hemispherical lens, which was used to slide against the PDMS-grafted glass surface. The PDMS-grafted glass surface was attached to a cantilever spring. After this glass slide was brought into contact with the spherical nub of the elastomer, a quick lateral displacement was given to the spring, which dragged the lens over the grafted PDMS surface until the spring recovered its neutral position. The drag force acting on the lens was measured from the deflection of the mechanically calibrated cantilever spring. Interfacial shear stress was calculated by dividing the drag force with the contact area.

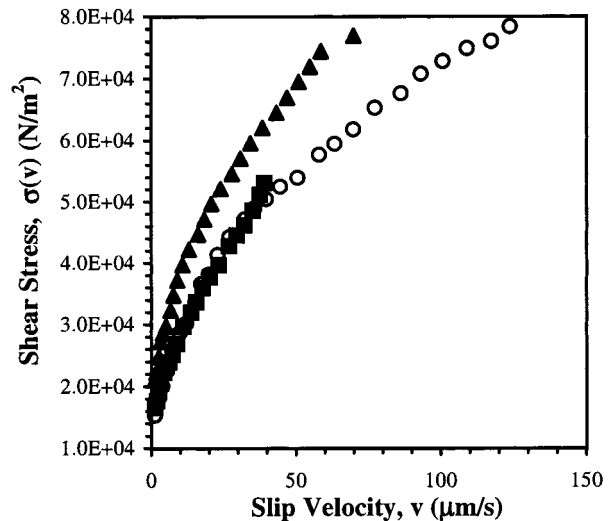


**Figure 8.** The interfacial shear stress between an elastic PDMS ribbon and a PDMS grafted glass surface increases as the ribbon is stretched. The shear stress in the direction of stretching ( $\blacktriangle$ ) is about 30% higher than the values obtained with unstretched ( $\circ$ ) film. The shear stress, perpendicular to the stretching direction ( $\blacksquare$ ), is almost the same as that of the unstretched elastomer.

are due to the differences in the mechanical constraints in the two systems. When the elastomer stretches in contact with glass, it also contracts laterally. To stretch over the glass slide, the elastomer must overcome friction in two mutually perpendicular directions. Thus, the effective frictional stress (eq 6) is expected to be higher than its value estimated from the sliding measurements.<sup>35</sup>

There are also other possibilities to consider. For example, the stretching itself may affect friction. This hypothesis gains support from an experiment we conducted, in which a prestretched elastomeric strip was slid over a PDMS-grafted glass. The shear stress, in this case, is found to be (30%) higher in the direction of stretching than against it. The amount of stretching (35%) of the elastomer in this experiment is, however, significantly higher than that encountered in the peel studies (<12%). Thus, stretching alone is not enough to explain the differences in the shear stresses measured in the peel and

(35) This lateral contraction was indeed evident in our studies from the displacements of the fluorescent particles. Detailed analysis of the energy dissipation due to such an effect is in progress.

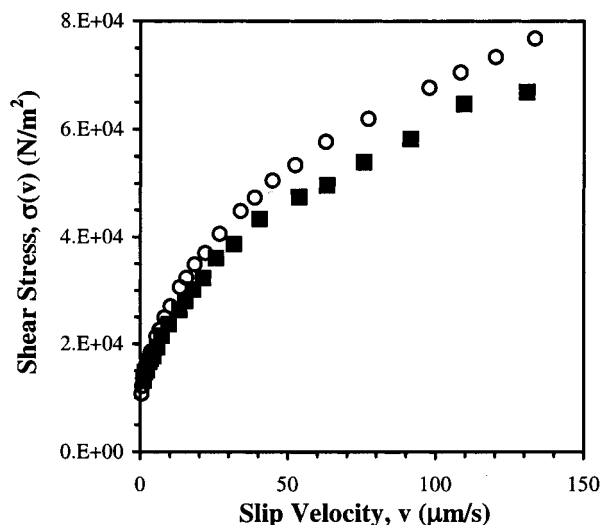


**Figure 9.** Interfacial shear stress of a monolayer of hexadecylsiloxane supported on an oxidized PDMS lens against a PDMS-grafted glass slide (■). In this case, the interdigitation between the PDMS polymer chains and the slider is eliminated, but the  $\sigma(v) \sim v$  profile is found to be only slightly smaller than that of the unmodified elastomer/PDMS interface (○).

sliding experiments. The effects of constraints as mentioned earlier must be considered. It has been suggested that frictional resistance to sliding is the effect of dislocation propagating<sup>36–38</sup> throughout the whole area of contact. It may be anticipated that the differences in mechanical constraints will contribute to the way dislocations nucleate and propagate. Even though we do not have a protocol to address this problem rigorously, it appears that the associated correction factor is simple because identical velocity exponents ( $\sim 0.36$ ) are found for the shear stresses in both the peel and sliding experiments.

In a previous publication,<sup>15</sup> we reported the values of the shear stress and the velocity exponent of an acrylic adhesive/PDMS interface ( $\sigma$  (Pa) = 13 000  $v^{0.35}$ ,  $v$  in  $\mu\text{m/s}$ ), which are almost the same as those ( $\sigma$  (Pa) = 12 000  $v^{0.37}$ ) of a PDMS elastomer on a PDMS film. Since the solubility parameter of the acrylic adhesive is quite different from that of PDMS, penetration of the PDMS chains into the bulk of the adhesive is an unlikely event. Based on the similarity of the shear stresses in both cases, it appears that the penetration of PDMS chains in a PDMS network does not play any major role in their frictional properties. We have established this point more strongly by measuring the interfacial shear stress of a close-packed monolayer of hexadecylsiloxane ( $\text{CH}_3(\text{CH}_2)_{15}\text{SiO}_{3/2}$ ) supported on an oxidized PDMS lens against a PDMS-grafted glass slide. Although the possibility of interdigitation is almost nil, the  $\sigma(v) \sim v$  profile for this system is found to be only slightly lower than that of the unmodified elastomer/PDMS interface (Figure 9).

**Estimation of Fracture Energy.** The frictional component of the energy dissipation in a steady-state peel experiment can be calculated by integrating the stress power,  $\sigma(v)v$ , as follows:<sup>15</sup>

$$G_0 = \frac{1}{V} \int_0^\infty \sigma(v) v dx \quad (14)$$

At very low peel angles, the experimental fracture energy

estimated from the overall energy balance is given by the first term on the right-hand side of eq 5, i.e.

$$G \approx \frac{P^2}{2Eh} \quad (15)$$

It is straightforward to show that eqs 14 and 15 are identical. Using eqs 6, 7, and 9, eq 14 can be integrated to yield

$$G \approx \frac{Eh}{2} \left( \frac{\partial u}{\partial x} \right)_{x=0}^2 \quad (16)$$

Substitution of the boundary condition,  $P/h = E(\partial u/\partial x)_{x=0}$ , into eq 16 recovers eq 15.

It is interesting to note that the elastic stretching component of the fracture energy ( $P^2/2Eh$ ) corresponds exactly to the frictional energy dissipation per unit extension of the crack area. By analogy, the second term ( $P(1 - \cos \theta)$ ) of the right-hand side of eq 5 corresponds to the opening mode component of the fracture energy. Although this separation of fracture energies makes sense in a qualitative way, the actual relationship between the opening and the shear mode components of the fracture energy is more involved because the stress intensity factor, in general, is a complex quantity,<sup>16</sup> i.e.,  $K = K_I + iK_{II}$  ( $i = \sqrt{-1}$ ).

We now estimate the frictional component of the fracture energy by rewriting eq 14 as follows:

$$G_0 = kV^n \int_0^\infty \left| \frac{\partial u}{\partial x} \right|^{1+n} dx \quad (17)$$

To evaluate  $G_0$  from eq 17, we need to know how the shear stress varies with velocity. The desired relationships were established in the previous sections in two ways—one directly from the peel experiment and the other from the hemispherical lens sliding measurements.  $G_0$ , estimated from the shear stresses obtained from the peel experiments, is in excellent agreement with the experimental fracture energies at a peel angle of  $5^\circ$  (Figure 10). This agreement re-enforces our view that the energy dissipated by friction can be a major contributor to the total fracture energy in elastic systems. As expected, the shear stresses obtained from the sliding experiments underestimate the fracture energy by about 50%. In the rest of this paper, we will use the  $\sigma(v)$  values obtained from the peel measurements to compute the frictional contribution to the total fracture energy.

Calculation of the frictional energy dissipation at a  $40^\circ$  peel angle, however, shows that it contributes about 35% of the total fracture energy (Figure 10). The discrepancy cannot, however, be explained with the thermodynamic work of adhesion, which is only about 47  $\text{mJ/m}^2$ . Attempts to measure the opening mode component of the fracture energy of this system, using rolling contact mechanics,<sup>39–40</sup> provide evidence that there may be other sources of energy dissipation in the system. The particular experiment is conducted by rolling a hemicylindrical PDMS rubber on the PDMS-grafted glass slide at different velocities. When a hemicylinder is first brought into contact with glass, a rectangular deformation develops in the zone of contact, the width of which increases as the cylinder rolls. Rolling of a cylinder can be viewed as the propagation of two mode-I cracks, one opening at the trailing edge and the other

(36) Briscoe, B. J.; Evans, D. C. B. *Proc. R. Soc. London* **1982**, A380, 389.

(37) Johnson, K. L. *Proc. R. Soc. London* **1997**, A453, 163.

(38) Chaudhury, M. K. *Curr. Opin. Colloid Interface Sci.* **1997**, 2, 65.

(39) Barquins, M. *J. Nat. Rubber Res.* **1990**, 5, 199.

(40) She, H. Q.; Malotky, D.; Chaudhury, M. K. *Langmuir* **1998**, 14, 3090.

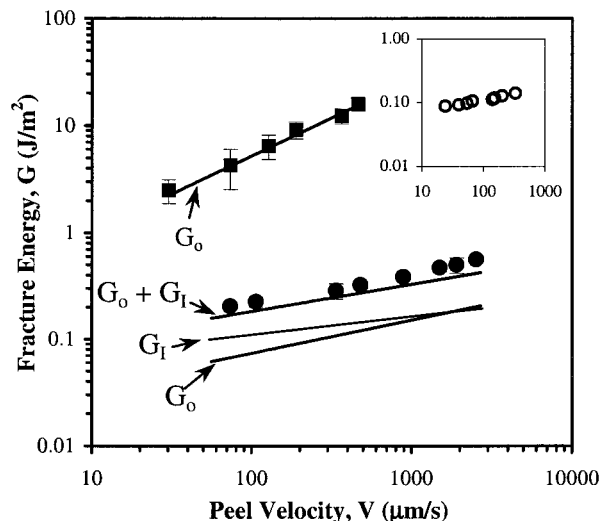


**Figure 10.** Fracture energies of PDMS elastomer on PDMS-grafted glass slide. ■ and ● denote the fracture energies at 5° and 40° peel angles, respectively, as calculated using eq 5. The frictional energy dissipation ( $G_0$ ) per unit extension of crack area was estimated using eq 17. At the 5° peel angle, almost all the fracture energy is contributed by frictional dissipation. At 40° peel angle, frictional dissipation accounts for 35% of the total fracture energy; the rest of the energy comes from the opening mode component ( $G_I$ ). The inset shows the opening mode component of the fracture energy (○) obtained by rolling contact mechanics up to a crack speed of 350  $\mu\text{m/s}$ .  $G_I$  values at higher speeds were obtained by extrapolation.

closing at the advancing edge. The energy associated with the opening of the crack can be estimated as follows:<sup>40</sup>

$$W_r = W_a (2(b/b_0)^{1.5} - 1)^2 \quad (18)$$

where  $W_a$  is the thermodynamic work of adhesion associated with the crack closing and  $b_0$  and  $b$  are the contact widths before and after rolling occurs.

The value of  $W_r$ , as measured from the rolling contact mechanics, increases from 85 to 130  $\text{mJ/m}^2$  as the crack velocity increases from 30 to 300  $\mu\text{m/s}$ . Evidently, some energy dissipation is associated with the mode-I fracture, the origin of which is not clearly understood. These  $W_r$  values when added to the frictional energy dissipation ( $G_0$ ) account for the total fracture energy at a 40° peel angle (Figure 10).

In the above fracture experiments, the elastomer is subjected to some amount of tensile deformation, where it is easy to see how a shear stress arises at the interface. In general fracture problems, however, shear stresses develop due to more subtle causes, an example of which is given below.

**Mixed Mode Fracture under Constraint.** When a thin plate is bent, one of its surfaces contracts and the other expands. The neutral plane lies between the two surfaces. Now, consider a thin adhesive in contact with a flat substrate, with its other surface constrained by a flexible but nonextensible backing. When a bending stress is applied to this adhesive, its constrained side cannot contract or expand, but its other surface tends to stretch, thus creating a shear stress at the adhesive-substrate interface (Figure 11). Many practical adhesives are designed to have such constraints. To test the contribution of this shear stress to fracture, an elastomeric PDMS film was peeled from a PDMS-grafted surface, with one of its surfaces constrained by a polymer tape. Since the elastomer cannot undergo a tensile deformation, but only bending, the adhesive fracture energy can be calculated

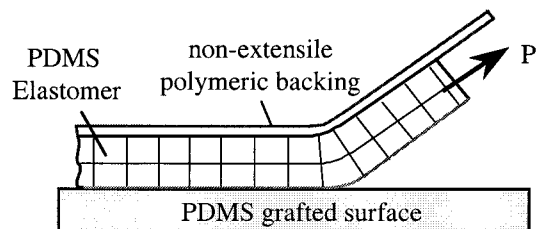


**Figure 11.** Sketch of an elastic film that is constrained on one side by a flexible but nonextensible polymeric backing. When the film is bent, the constrained side of the film cannot contract or expand, but the other surface tends to stretch, thus creating shear stress as well as slippage at the adhesive-substrate interface.

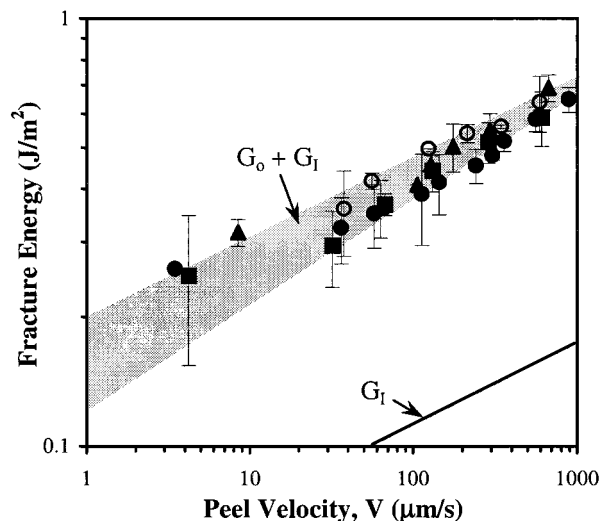


**Figure 12.** Experimentally measured fracture energies of a PDMS elastomer from a PDMS-grafted glass surface when the free surface of the elastomer is constrained with a polymeric tape. ■, ●, ▲, and ◇ denote the peel angles of 5, 10, 20, and 40°, respectively. Here, 75% of the fracture energy is contributed by the frictional energy dissipation.

by the second term of eq 5. The results are shown in Figure 12. Note that the peel fracture energies obtained at different peel angles are roughly similar to each other at a given peel speed—so are the slip displacements (10–12  $\mu\text{m}$ ) (Figure 13). The total fracture energy was calculated as a sum of two contributions: one is the frictional dissipation (eq 17), and the other is the opening mode component of the energy, obtained via contact mechanics. The experimental fracture energies are in fair agreement with the values estimated by the above method. Here, the frictional dissipation contributes about 75% of the total fracture energy, thus proving conclusively that the crack does not propagate without overcoming some frictional resistance at these asymmetric interfaces.

### Final Remarks

We have reported several case studies that clearly demonstrate that friction plays a very important role in the fracture of asymmetric interfaces. Since the interface of the PDMS elastomer and the grafted PDMS film exhibits kinetic friction, the fracture problem reduces to that of a crack moving in a viscoelastic medium—there are, of course, some apparent differences. In viscoelastic cases, the crack driving force ( $G - W_a$ ) can be expressed as the product of the work of adhesion ( $W_a$ ) and a viscoelastic dissipation function ( $\Phi$ ). In the current triboelastic situation, however, the term contributing to the frictional drag is related to  $W_a$  in such a complex manner that it

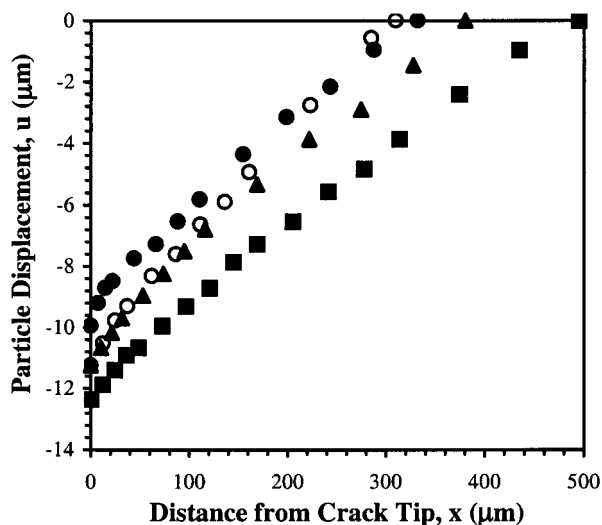


**Figure 13.** Typical slip displacements of fluorescent particles measured when the elastic film is constrained at its free surface. ■, ●, ▲, and ○ denote the peel angles of 5, 10, 20, and 40°, respectively, at a peel velocity of 125  $\mu\text{m/s}$ . The average slip displacements at various peel angles are in the range 10–12  $\mu\text{m}$ .

becomes difficult to decouple  $W_A$  and  $\Phi$  in a meaningful way. If, indeed, such a decoupling is possible, then  $W_A$  should be a rate dependent quantity because the interface exhibits shear thinning behavior.

Finally, it may be asked how general the effect of interfacial friction on the fracture of asymmetric interfaces is. Although interfacial shear stress is quite high in most polymers, the frictional dissipation may still be significant. To illustrate this point, let us consider an example in which the average interfacial shear stress ( $\sigma$ ) is about  $10^8 \text{ N/m}^2$  and the average slip displacement ( $u$ ) of the crack tip is only about 100 Å. In this case, the frictional work ( $\sigma u$ ) per unit extension of crack area is about 1  $\text{J/m}^2$ , which is considerably higher than the thermodynamic work of adhesion ( $\leq 0.1 \text{ J/m}^2$ ) in many polymeric systems. Thus, the frictional energy dissipation may be a significant contributor to the total fracture energy. Clearly, slip experiments affording much higher resolution than that used here are needed to answer the above question in a decisive way. In the absence of interfacial slip, however, shear stress is distributed in the bulk of the polymer, causing viscoelastic or plastic deformation, which can also increase energy dissipation in many systems.

### Experimental Section

**General Information.** The fluorescent latex particles used for this study were purchased from Molecular Probes Inc., Eugene, OR. The as-received particles (0.5  $\mu\text{m}$  [L5261]) were colloidal dispersions in water that were free of surfactants. The excitation and emission wavelengths of the particles were 490 and 515 nm, respectively. Hydrido-functional PDMS of a number average molecular weight of 11 080 and a polydispersity index of 1.17 was received as a gift from Dow Corning Corp., Japan Division. The materials for preparing the silicon rubber were supplied to us by Dow Corning as a commercial kit, Dow Corning Sylgard 184. The microscope used to examine the fluorescent particles was a Nikon Diaphot inverted microscope that had an epifluorescent attachment.

**Grafting of PDMS on Glass.** Poly(dimethylsiloxane) (PDMS,  $\text{CH}_3\text{CH}_2\text{CH}_2\text{CH}_2(\text{OSi}(\text{CH}_3)_2)_n(\text{CH}_3)_2\text{SiH}$ ) was grafted onto glass microscope slides according to the following method. The glass slides were first cleaned by hot piranha solution, rinsed with copious amounts of water and then dried by blowing pure nitrogen over it. These slides were later briefly oxidized by an oxygen plasma in a Harrick plasma cleaner for about 30 s at the lowest

power setting. The clean glass slides were then reacted with the vapor of undecenyltrichlorosilane according to a method described previously.<sup>41</sup> The silane reacted with the glass surface and formed an adsorbed monolayer bearing terminal olefin (vinyl) groups. Hydrido-functional PDMS was reacted with the olefin group by a platinum-catalyzed hydrosilation reaction for about 20 h. The PDMS-grafted glass slides were then cleaned with chloroform in a Soxhlet extractor to remove unreacted polymer. Although we could not measure the thickness of the grafted layer on glass, the thickness of a similar layer on a silicon wafer was found to be about 100 Å.

**Preparation of the PDMS Elastomeric Sheets, Hemicylinders, and Hemispheres.** Thin ( $\sim 0.76 \text{ mm}$ ) sheets of PDMS elastomer [Dow Corning Syl-184] were prepared from a reactive mixture of a vinyl-terminated PDMS ( $\text{CH}_2=\text{CH}(\text{Si}(\text{CH}_3)_2\text{O})_m\text{Si}(\text{CH}_3)_2\text{CH}=\text{CH}_2$ ), a methyl-hydrogen siloxane cross-linker ( $\text{CH}_3(\text{SiHCH}_3\text{O})_p(\text{Si}(\text{CH}_3)_2)_r\text{CH}_3$ ), and a platinum catalyst, according to the methodology prescribed for this commercial polymer. The mixture was poured onto a polished silicon wafer whose surface was modified by a perfluorotrichlorosilane monolayer ( $\text{CF}_3(\text{CF}_2)_7(\text{CH}_2)_2\text{SiCl}_3$ ). The polymer was first cured at room temperature overnight and then heated to 70 °C for 3 h inside a clean polystyrene Petri dish. The cured elastomers were then cleaned with chloroform using a Soxhlet extractor in order to remove the unreacted oligomers. The samples were used after allowing all the chloroform to evaporate completely. The dry elastomer was stored inside a desiccator. The elastic modulus of the elastomer was obtained by measuring its stress-strain behavior under tensile deformation.

The detailed method for preparing the PDMS hemicylinders and hemispheres have previously been described in refs 41 and 42. Here only a brief description is given. The same mixture of the vinyl-terminated PDMS and siloxane cross-linker was applied onto the surfaces of fluorocarbon-treated glass cover strips (3 mm  $\times$  60 mm) using a microsyringe. The liquid polymer was contained within the strip and set to elastomer in the shape of hemicylinder. Hemispheres were made by placing small drops of the same mixture on the fluorinated microscope glass slides. These hemicylinders and hemispheres are cured and cleaned in the same way as the elastomeric sheets.

**Peel Experiment.** Smaller strips (50 mm  $\times$  12 mm  $\times$  0.76 mm) of the PDMS elastomers were cut out of the larger sheets. The surface of the elastomer, which was cured against the silanized silicon wafer, was gently placed over the PDMS-grafted glass slide in order to avoid prestress. The elastomer was peeled from the glass at different angles with a string that ran over a pulley. Peel velocities were controlled by hanging different dead loads on the free end of the string. At each load, peel velocities were averaged from at least four data sets. The peeling process was viewed through a microscope and videotaped. Detailed analysis of the peel data was done with the aid of a desktop computer.

**Estimation of Slip Profile.** Slippage of the elastomer on PDMS-grafted glass slide was measured using a particle tracking experiment described previously.<sup>15</sup> Here, a brief description is given. Small (0.5  $\mu\text{m}$ ) fluorescent particles were sprinkled onto the surface of the elastomer that contacted the glass during peel measurements. The excitation and emission wavelengths of the particles were 490 and 515 nm, respectively. The fluorescent particles were excited with UV light emitted from a mercury lamp through the epifluorescent port of the microscope. The particles were observed with a CCD video camera, and their motions were videotaped. Later, the motion of the fluorescent particles was analyzed in detail using a desktop computer.

**Interfacial Shear Stress Measurement.** The first method used to determine the interfacial shear stress as a function of slip velocity is similar to that used by others.<sup>8,29–31</sup> A PDMS elastic hemisphere lens was adhered to a flat glass surface that was attached to the end of a cantilever spring, whose position could be adjusted with a  $x$ - $y$ - $z$  micromanipulator. Using the micromanipulator, the PDMS lens was first brought down into contact with the PDMS-grafted surface. Following the method

(41) Chaudhury, M. K.; Whitesides, G. M. *Langmuir* **1991**, *7*, 1013.

(42) Chaudhury, M. K.; Weaver, T.; Hui, C.-Y.; Kramer, E. J. *J. Appl. Phys.* **1996**, *80*, 30.

used by Brown,<sup>8</sup> a quick lateral displacement was given to the spring, which dragged the lens over the glass slide until the spring recovered its neutral position. The drag force acting on the lens was measured from the deflection of the mechanically calibrated cantilever spring. Interfacial shear stress was calculated by dividing the drag force with the contact area. The contact area changed only slightly (<1%) during the entire sliding process.

In the second (modified) method, a small PDMS lens ( $R = 0.60$  mm) was first placed on a clean glass slide. The lens was covered with the same elastomer film as that used for the peel measurements (Figure 7). The whole system was then subjected to a low pressure that ensured the flat elastomer to adhere well to the glass slide. The central part of the elastomer film formed a spherical bump just above the hemispherical lens, which was slid against the PDMS-grafted glass surface. In this case, the PDMS-grafted glass surface was attached to the cantilever spring, while the elastomer sheet and the glass slide were attached to another  $x$ - $y$ - $z$  micromanipulator. After the PDMS-grafted glass slide was brought into contact with the spherical bump of the elastomer film, shear stresses were measured according to the procedure described above.

The surface used for the sliding experiment under stretching was prepared as follows. A small PDMS elastomeric lens was first placed onto a glass slide, which was later covered with a PDMS elastomer that had already been stretched to about 35%

of its original length. After the elastomer made good contact with the glass slide, its ends were clamped down by adhesive tapes. The elliptical dimple that was produced on the elastomeric sheet above the lens was used to measure friction against the PDMS-grafted glass slide.

**Mode-I Fracture Energy Measurement.** The value of mode-I fracture energy,  $G_i$ , was obtained from rolling contact mechanics. The rolling experiment was performed under a microscope with reflection optics. A small (length = 2 mm,  $R = 2.5$  mm) hemicylinder with its flat side adhered to a thin glass plate was brought into contact with the PDMS-grafted surface with the help of a micromanipulator. The PDMS-grafted glass surface rested on an analytical balance (Mettler) so that any change of load during rolling could be measured. The cylinder was rolled by tilting one of its edges with the micromanipulator, controlled by an electrical motor. The rolling speed was varied by changing the motor speed. The entire rolling process was videotaped, and the subsequent analysis was carried out with a desktop computer.

**Acknowledgment.** This work is based on an important suggestion by Professor P. G. de Gennes. Financial support from Dow Corning Corp. and the Office of Naval Research are gratefully acknowledged.

LA980290L